INTERNATIONAL JOURNAL OF AUTOMOTIVE AND MECHANICAL ENGINEERING (IJAME)
ISSN: 2229-8649 e-ISSN: 2180-1606
VOL. 20, ISSUE 1, 2023, 10258 – 10273
DOI: https://doi.org/10.15282/ijame.20.1.2023.08.0793

ORIGINAL ARTICLE

Energy and Exergy Investigation of a Solar Air Heater for Different Absorber Plate Configurations

Mustafa J. A-Dulaimi[1,*], Areej H. Hilal[1], Husam A. Hasan[2,3], and Faik A. Hamad[4]

[1]Department of Air Conditioning, Al Esraa University College, 10069, Baghdad, Iraq
[2]Department of Studies, Planning & Follow-up, Ministry of Higher Education & Scientific Research,10060 Baghdad, Iraq
[3]Electromechanical Engineering Department, University of Technology, 10066, Baghdad, Iraq
[4]School of Science & Engineering, Teesside University, Middlesbrough, TS1 3BA, UK

ABSTRACT – In this paper, the effect of using different configurations of absorber plate, including one line finned flat absorber and two lines finned absorber plate, on the thermal performance of a flat plate – double passing solar air heater was investigated experimentally. L- shape fins are soldered on the absorber plate to roughen the absorber plate and generate vortices to enhance the heat transfer between the working fluid (air) and absorber plate to improve the thermal efficiency. The outdoor experimental test was carried out during February and May under the weather conditions of Baghdad city (Longitude 33.3 N and Latitude 44.44 E). The results show that the air temperature is 48 °C, 47.5 °C, and 58.5 °C at an air velocity of 1.7 m/s for a single line of fins which increased to 52 °C, 57.5 °C, and 66 °C at air velocity of 0.9 m/s for two lines of fins. The efficiency is increased by 28% for one line of fins and 66% for two lines of fins at an air velocity of 0.9 m/s while increased by 27% for one line of fins and 51% for two lines of fins at an air velocity of 1.7 m/s. The average exergy destruction rate increases by 37.6%, 60.6%, and 68.66% for the absorber plate, working fluid, and glass cover, respectively, for velocity increase from 0.9 m/s to 1.9 m/s. The exergy efficiency increased by 24.1% when the velocity increased from 0.9 m/s to 1.9 m/s.

ARTICLE HISTORY
Received: 09th Jan 2022
Revised: 29th Dec 2022
Accepted: 15th Feb 2023
Published: 31st Mar 2023

KEYWORDS
Double-pass solar air heater;
Thermal performance;
Flat solar air heater;
Thermal efficiency;
Finned surface

NOMENCLATURE

A	Cross section area of the solar heater pass
A_B	Bottom wall surface area (m^2)
A_E	Side walls surface area (m^2)
A_p	Absorber plate area (m^2)
D_h	Hydraulic diameter of the inlet of SAH (m)
$h_{r,g-sky}$	Radiation heat transfer coefficient between glass and sky (W/m^2. K)
$h_{c,g-amb.}$	Convection heat transfer coefficient between glass and surrounding (W/m^2. K)
$h_{r,p-g}$	Radiation heat transfer coefficient between absorber plate and the glass (W/m^2. K)
$h_{c,p-g}$	Convection heat transfer coefficient between absorber plate and the glass (W/m^2. K)
I	Solar intensity (W/m^2)
K_{insu}	Thermal conductivity of the insulation (W/m. K)
k_{air}	Thermal conductivity of the air (W/m. K)
L	Length of the solar air heater (m)
$\dot{m}$	Air mass flow rate inside the solar air heater (kg/s)
Nu	Nusselt number
Q_{gain}	Useful heat gain (W)
Q_{losses}	Heat loss (W)
T	Temperature (°C)
$T_{amb.}$	Ambient temperature (°C)
T_{dp}	Dry bulb temperature (°C)
T_g	Glass temperature (°C)
T_{out}	Fluid outlet temperature (°C)
T_p	Absorber plate temperature (°C)

*CORRESPONDING AUTHOR | Mustafa J. A-Dulaimi | ✉ mustafa@esraa.edu.iq

T_{in}	Fluid inlet temperature (°C)
T_s	Sun temperature (°C)
T_{sky}	Sky temperature (°C)
U_E	Heat transfer coefficient from side walls (W/m^2.k)
U_B	Heat transfer coefficient from bottom wall (W/m^2.k)
U_F	Heat transfer coefficient from top (W/m^2.k)
U_T	Total transfer coefficient (W/m^2.k)
v	Air velocity at the inlet of the solar air heater (m/s)
V_w	Wind speed (m/s)
ρ	Air density (kg/m^3)
η	Thermal efficiency

INTRODUCTION

Energy demand has increased dramatically during the past three decades due to the global population increase and the significant increase in energy consumption in modern life and industry. It is well known that the increase in using of traditional energy sources (fossil fuels) will greatly affect the level of pollution, global warming, and energy prices. To control these effects, solar energy, which is a sustainable renewable energy source, has become an important topic of research. It is characterized by being a major source of green energy, free of cost, and sustainable [1-2]. Recent studies [3-6] have concluded that system development to improve thermal energy conversion performance is a fertile topic of research with many beneficial applications worldwide. Energy efficiency improvements can also be achieved in industrial product development processes by increasing the surface area of heat exchange by inserting fins, baffles and turbulators, which also generate turbulence. Another method to improve the efficiency which includes thermal fluids with increased thermophysical properties of nanofluids. The traditional fluids utilized in the applications of heat transfer were replaced by nanofluids, which were considered to be of high capacity due to their high thermal conductivity [7]; they are commonly utilized in the applications of heat transfer for the purpose of increasing the energy effectiveness of numerous devices [8-10]. Different types of thermal solar collectors can be employed to convert solar radiation into thermal energy for heating and cooling applications. Solar air heaters (SAH) are solar panels that convert solar energy into thermal energy usable in the form of hot air to warm homes or to dry agricultural crops. SAHs are distinguished with low manufacturing cost, simplicity, and hazardless to health and environment. There's a wide variety of designs SAH designs that are classified according to the airflow inside them with a single- and double-pass.

Many researchers have examined the development of the thermal performance of heat systems using fins, baffles and turbulator. Kumar [11] experimented the friction characteristics and heat transfer under laminar flow conditions for surface-modified solar air heaters. A roughened V-corrugated absorber plate and roughened inner surface of a rectangular duct were used. According to the results, the modified absorber plate exhibits a higher heat transfer rate with higher friction loss. Jia [12] investigated the influence of air volume flow rate and irradiance of a modified solar air heater with a folded spoiler on the absorber plate. The modified solar air heater has been determined to be more effective than the conventional one. Abdullah [13] conducted an experimental investigation to determine the effect of exterior mirrors and aluminum cans tabulators on the performance of a single-pass SAH. Three distinct designs of absorber plates were tested, namely: smooth plate, cans-line roughened plate and staggered-cans roughened plate. Air guide vanes were fixed at the inlet The efficiency enhancement was found to be 73%. Dezan [14] investigated the effect of winglets pairs on the performance of a SAH. The examined parameters were: the chord length, angle of attack, and the height of winglets. It was concluded that the friction factor is more sensitive than the Nusselt number to tested variables. Jouybari [15] tested the effect of coating on the absorber plate of a SAH with a thin porous media layer. It was found that the thin porous layer improved the thermal performance by 500% and increased the friction loss by 200%. Hassan [16] conducted an experimental investigation to examine the performance of a tubular solar heater (TSAH) with an absorber in the shape of sheet of adjacent tubes. The results revealed that the efficiency and the air temperature of the modified tubular solar heater are higher by 132% and 13 °C as compared with conventional SAH. Wang [17] developed a SAH roughened with S-shaped ribs with gaps. The results showed that the roughened SAH has improved thermal efficiency by 13% to 48%. Ghritlahre [18] investigated experimentally the thermal performance of arc-shaped roughened solar air heaters with apex up and apex down airflow. Tests were performed with airflow rates ranging from 0.007 to 0.022 kg/s. The results showed that efficiency improved with increased airflow rates, which reached 73.2% at the apex upstream flow and 69.4% at the apex downstream flow at a mass flow rate of 0.022 kg/s. Yassien [19] compared the performance of two triple-pass SAHs. The first one has a double glass cover, and the other has tubes network under the absorber plate. The results showed that the first model has a higher efficiency than the second model at 80.2% and 73.4%, respectively. Baissi [20] explored the effect of perforation of delta-shaped baffles on the performance of a SAH. The results showed using baffles led to an increase in heat transfer. The maximum thermal enhancement factor (TEF) rate of 2.26 and 2.21 was achieved for perforated and non-perforated baffles, respectively. Ranjbar [21] investigated numerically, the effect of roughened absorber plate with rectangular, triangular and elliptical fins on the performance of a SAH for different inclination angles. It was found that the efficiency of SAH with rectangular fins is higher than that with elliptical and triangular fins by 12.5% and 5.5%, respectively. Also, the optimum angle was reported between 50° and 70°. Saravanan et al. [22] examined

experimentally the performance of a solar air heater roughened with perforated and non-perforated C-shape fins. It was found that using perforated fins increases the heat transfer rate by 2.67.

The effect of using nanofluids in SAH also was investigated by many researchers. Olia [23] investigated the effect of volume of the base fluid on the thermal performance and entropy generation of parabolic trough collectors (PTCs). It was found that nanofluids augment heat transfer and thermal efficiency, and they can reduce the entropy generation in the system, but they work to increase the pressure drop. The thermodynamics of the turbulent flow of the nanofluid in a solar heating channel with the roughness of the rib on the absorber plate was analyzed by using the second law of thermodynamics [24]. Effects of various factors, namely: friction, the concentration of nanofluid on thermal reflections, Reynolds number, angle, height, and degree of rib used on the absorbing plate, were studied. The results show that the use of nanofluids with a concentration of 0.04 led to a decrease in the generation of thermal entropy by about 11.1%. Also, increasing the rib height in the range 0.025-0.033 for Re = 3200 decreased the thermal entropy generation by about 21.05%. In [25], a study of pulsed flow in a 3D channel was presented; the turbulent and laminar flows inside the channel were tested. The effect of different geometries of the transverse channel, such as triangle, hexagon and circular with pulsed flow was also studied. Alumina nanofluids (Al_2O_3) were used as a working fluid in various proportions (0 percent [pure water], 3 percent, and 5 percent) to demonstrate its effect on pressure, velocity and temperature. Results showed that Al2O3 could provide energy at a constant temperature when there is an increase in the percentage volume of liquid.

The literature review indicated that there are many research activities in the field of improving the performance of solar air heaters. In spite of these research activities and a large number of published papers but there is room for further improvement of the solar air heaters performance for the local weather conditions in Baghdad, Iraq. The significance of this research is due to its contribution to reducing the greenhouse effect and the wide range of its applications. Therefore, the aim of this paper is to investigate the effect of the inlet air velocity and L shape fins on the efficiency of the solar air heater. To achieve this aim, a set of experiments were conducted for a number of days in 2019, from February to May, under clear sky conditions. The data were collected every hour for 10 hours/day. Three air velocities of 1.9 m/s, 1.7 m/s, and 0.9 m/s were recorded

EXPERIMENTAL SETUP

The experimental setup used in the present study was designed, built and installed on the roof of Al-Esraa university college, Baghdad, Iraq (33.3 N longitude and 44.44 E latitude). The experimental setup is a double-pass solar air heater, as shown in Figure 1 and 2. The solar air heater consists of a rectangular box made from PVC sheets of thickness 2 mm. The inner dimensions of the solar heater are 90×50.5×16 cm. The interior sides of the solar heater are insulated with two layers of cork and ArmaFlex of thickness 2 cm and 1 cm, respectively, to minimize the heat loss to the surroundings. The solar heater has a glass cover of 69×49 cm and 3 mm in thickness. The partition wall between the upper and lower channels of the solar heater is made of a copper flat absorber plate of 70×50 cm. The plate is painted black to increase its absorptivity for solar radiation. L shape copper fins are soldered to the upper face of the absorber plate.

First, six fins are soldered in a line for the first configuration, and then another six fins are soldered in a second line parallel to the first one, so the number of fins becomes 12 fins for the second configuration. The bottom of the solar heater, which is in the lower pass, is covered by an iron plate to receive the heat radiated from the lower face of the copper absorber plate and retransfer it to the air passing in the lower pass before leaving the solar heater. The air enters the heater through a special metallic diffuser of 45 cm in length. The diffuser has a circular inlet with a diameter of 7.5 cm and rectangular outlet with 50.5×8 cm. The air leaves the solar heater through a rectangular exit of 50.5×8 cm at the end of the lower pass. The air is supplied to the solar heater using a centrifugal blower connected to the diffuser through a rubber hose. The hose is insulated with a layer of thermal wool. The velocity of the air is controlled by an adjustable gate fixed at the suction port of the blower. Figure 3 shows the image of the experimental setup. The temperatures are measured by using six thermocouples type (K) connected to a data logger of type BTM-4208SD. Three thermocouples are used to measure the temperature of the absorber plate. Two thermocouples are used to measure the temperature of air at the inlet and outlet of the solar heater. One thermocouple is used to measure the inside temperature of the insulation. The wind velocity is measured using an anemometer. The solar radiation data for Baghdad is taken from the Iraqi Ministry of Science and Technology.

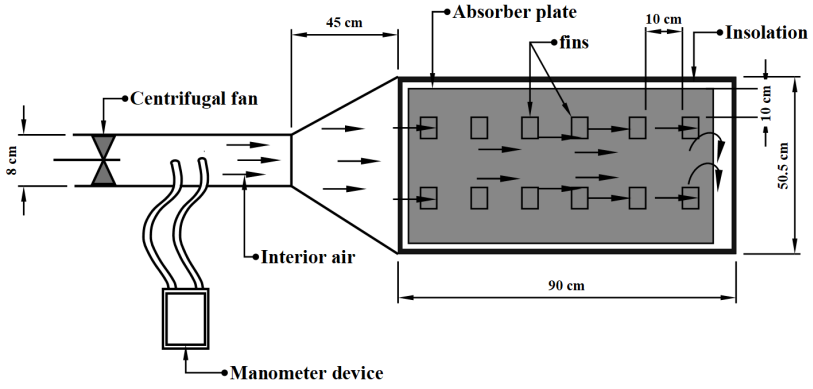

(a) top view

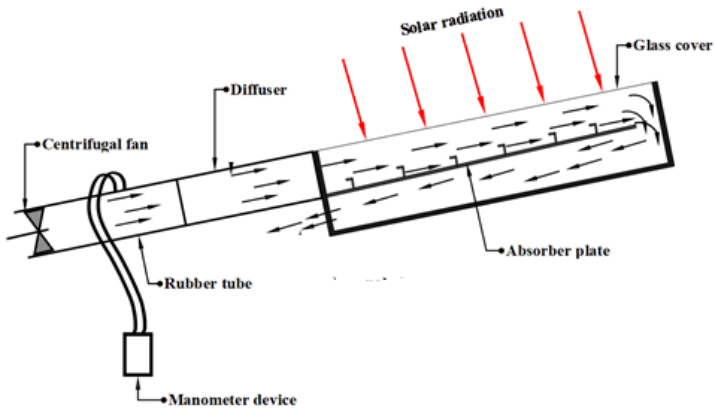

(b) side view

Figure 1. Experimental solar air heater system

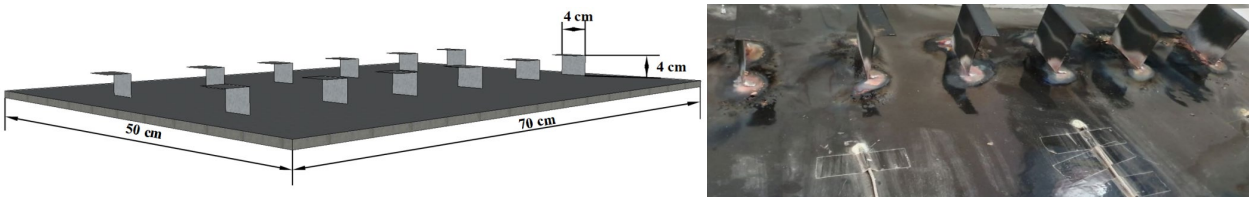

Figure 2. Absorber plate with fins

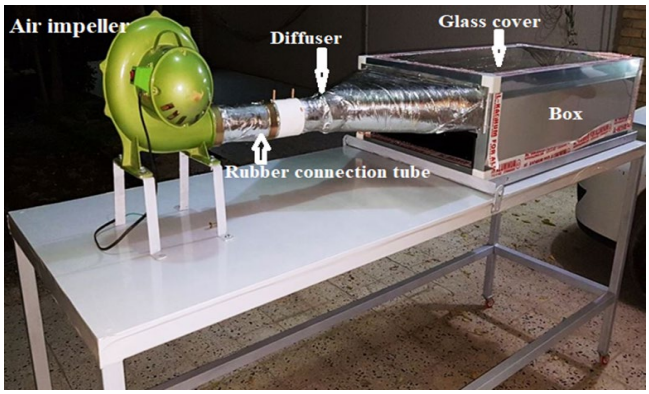

Figure 3. Test rig

THERMAL PERFORMANCE OF SOLAR AIR HEATER

The air velocity is varied for all experiments and temperatures are measured at the inlet and outlet of the flowing air and at different locations of the absorber plate. The heat balance of the solar air heater requires the calculations of heat input from solar radiation and the heat losses from the walls. Figure 4 shows the thermal resistance of the SAH used to compute the overall heat transfer coefficient. The heat transfer coefficient of the insulated side walls (edges) of the solar air heater (U_E) is in Eq. (1) [26]:

$$U_E = \frac{K_{insu} A_E}{L} \tag{1}$$

The heat transfer coefficient of the insulated bottom side wall of the solar air heater (U_B) [26] is:

$$U_B = \frac{K_{insu} A_B}{L} \tag{2}$$

The heat transfer coefficient of the top side of the solar air heater (U_F) [26] is in Eq. (3):

$$U_F = \left[\frac{1}{h_{r,g-sky} + h_{c,g-amb.}} + \frac{1}{h_{r,p-g} + h_{c,p-g}} \right]^{-1} \tag{3}$$

The radiation heat transfer coefficient ($h_{r,p-g}$) between the absorber plate and the glass cover can be calculated by Eq. (4) [27]:

$$h_{r,p-g} = \frac{\sigma(T_p + T_g)(T_p^2 + T_g^2)}{\frac{1}{\varepsilon_p} + \frac{1}{\varepsilon_g} - 1} \approx \frac{4\sigma(T_p^2)}{\frac{1}{\varepsilon_p} + \frac{1}{\varepsilon_g} - 1} \tag{4}$$

The convection heat transfer coefficient from the absorber plate to glass cover ($h_{c,p-g}$) [26] is calculated by:

$$h_{c,p-g} = \frac{Nu.\, k_{air}}{D_h} \tag{5}$$

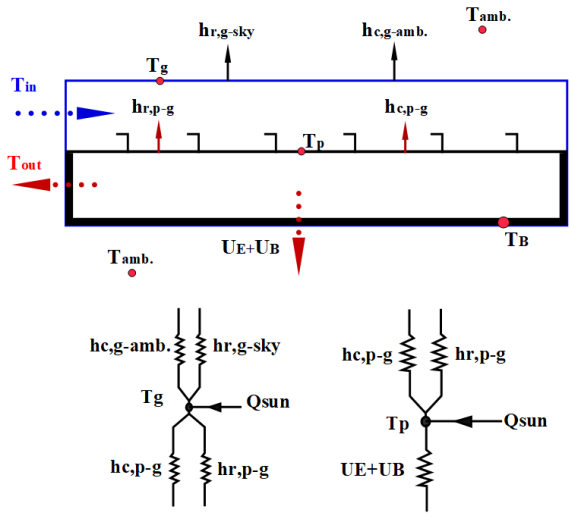

Figure 4. Heat transfer network and schematic of solar air heater thermal losses

Nusselt number of the solar air heater is calculated by Eq. (6) [26]:

$$Nu = 0.0158(Re)^{0.8} \tag{6}$$

The convective heat transfer coefficient of the wind at the outer surface of the glass cover ($h_{c,g-amb.}$) as presented in Eq. (7) and (8) [26]:

$$h_{c,g-amb.} = 2.8 + 3\, V_w \tag{7}$$

$$h_{c,g-amb.} = 5.7 + 3.8\, V_w \tag{8}$$

The radiative heat transfer coefficient between the outer surface of the glass cover and the sky ($h_{r,g-sky}$), it is given as Eq. (9) [28]:

$$h_{r,g-sky} = \varepsilon_g \sigma \left[(T_g + 273)^4 - (T_{sky} + 273)^4\right] / (T_g - T_{sky}) \tag{9}$$

Different models are available for the effective sky temperature. According to Duffie and Beckman [24], the sky temperature is determined as:

$$T_{sky} = T_{amb.}\left[0.711 + 0.0056T_{dp} + 0.000073T_{dp}^2 + 0.013\, cos(15t)\right]^{1/4} \tag{10}$$

where T_{sky} and $T_{amb.}$ (ambient temperature) are in (K), t is an hour from midnight. Alfegi et al. [29] gave the following equations for sky temperature:

$$T_{sky} = 0.0552(T_{amb.})^{1.5} \tag{11}$$

Or,

$$T_{sky} = T_{amb.} - 6 \tag{12}$$

Equations (11) and (12) are only applicable in humid climates. When the dew point temperature or relative humidity is available, Eq. (10) is utilized; otherwise, Eq. (11) is utilized. The total amount of heat lost from the SAH (U_T) [24] is:

$$U_T = U_F + U_E + U_B \tag{13}$$

Heat loss from The SAH (Q_{losses}) is calculated as follows [26]:

$$Q_{losses} = U_T A_h (T_p - T_{in}) \tag{14}$$

where A_h is the solar air heater upper surface area (m^2). The heat gain of the flowing air can be determined as follows [26]:

$$Q_{gain} = \dot{m} cp (T_{out} - T_{in}) \tag{15}$$

$$\dot{m} = \rho v A \tag{16}$$

The thermal performance of the solar air heater is related to the heat transfer from the absorber plate and the heat collection efficiency. The thermal efficiency of the solar air heater can be calculated as follows:

$$\eta = \frac{Thermal\ power\ transferred\ to\ fluid}{Thermal\ power\ received\ by\ absorber} \tag{17}$$

$$\eta = \frac{Q_{gain}}{I\ A_P} = \frac{\dot{m} cp (T_{out} - T_{in})}{I\ A_P} \tag{18}$$

EXERGY ANALYSIS OF THE SOLAR AIR HEATER

Exergy analysis applied to a solar collector aid in the creation of an optimal design and provides guidance on how to reduce exergy losses. The Exergy principle is one of two approaches to the second law analysis, with the other being entropy creation from irreversibilities. Both approaches provide essentially the same outcomes. Maximizing exergy efficiency can help to reduce the amount of exergy lost during thermodynamic processes. In an environment with a temperature of T_a, the optimum work may be done by transferring energy from a heat source with a temperature of T. Exergy with the amount of Ex_{heat} is always companion with heat transfer Q at a location at a thermodynamic temperature T [30]. The applied assumptions in this model are:

i. Steady flow operation.
ii. Steady-state heat transfer.
iii. The fluid is incompressible.
iv. Negligible the effects of kinetic and potential energy.
v. There are no nuclear or chemical reactions in the system.

$$Ex_{heat} = Q\left(1 - \frac{T_{amb.}}{T}\right) \tag{19}$$

where $\left(1 - \frac{T_{amb.}}{T}\right)$ is the Carnot coefficient factor. In general, Eq. (20) is implemented to derive the exergy balance of each element of the SAH [30,31]:

$$Ex_{in} - Ex_{out} - Ex_{accu} - Ex_{dest} = Ex_{sys} \tag{20}$$

Figure 5 shows the exergy exchange between the different components of the SAH [32, 33].

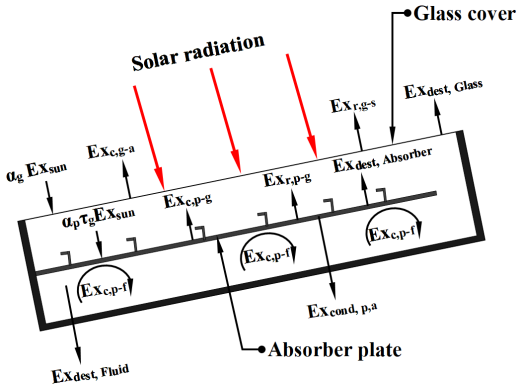

Figure 5. Exergetic flow diagram in solar air heater

Glass Cover Exergy

The exergetic balance of the glass cover is:

$$Ex_{\text{dest , Glass}} = \alpha_g Ex_{\text{sun}} + Ex_{r,p-g} + Ex_{c,p-g} - Ex_{c,g-a} - Ex_{r,g-s} \tag{21}$$

The sum of the exergy absorbed by the glass cover from the sun $(\alpha_g \text{Ex}_{\text{sun}})$ and the radiative $(Ex_{r,p-g})$ and convective exergy $(Ex_{c,p-g})$ transferred from the absorber plate to the glass cover represents the exergy gained by the glass cover. Part of the absorbed exergy is lost to the environment by convective $(Ex_{c,g-a})$ and radiative $(Ex_{r,g-s})$ exergy transfer, while the remainder is destroyed $(Ex_{\text{dest , Glass}})$. Ex_{sun} is the result of the Petela expression [32-34] and the incident solar radiation G.

$$Ex_{sun} = GS_g\left[1 + \frac{1}{3}\left(\frac{T_a}{T_s}\right)^4 - \frac{4}{3}\left(\frac{T_a}{T_s}\right)\right] \tag{22}$$

where T_s is the sun temperature and is ssumed to be 6000 K. $(Ex_{r,p-g})$ is the radiative exergy transferred from the abrorber plate to the glass cover and given by:

$$Ex_{r,p-g} = h_{r,p-g}S_g(T_p - T_g)\left[1 + \frac{1}{3}\left(\frac{T_a}{T_p}\right)^4 - \frac{4}{3}\left(\frac{T_a}{T_p}\right)\right] \tag{23}$$

$(Ex_{c,p-g})$ is the convective exergy transferred from the absorber plate to the glass cover and given by:

$$Ex_{c,p-g} = h_{c,p-g}S_g(T_p - T_g)\left(1 - \frac{T_a}{T_p}\right) \tag{24}$$

$(Ex_{c,p-g})$ is the convective exergy lost from the glass cover to the environment and given by:

$$Ex_{c,g-a} = h_{c,g-a}S_g(T_g - T_a)\left(1 - \frac{T_a}{T_g}\right) \tag{25}$$

$(Ex_{r,g-s})$ is the radiative exergy lost from the glass cover to the sky and given by:

$$Ex_{r,g-s} = h_{r,g-s}S_g(T_g - T_{sky})\left[1 + \frac{1}{3}\left(\frac{T_a}{T_g}\right)^4 - \frac{4}{3}\left(\frac{T_a}{T_g}\right)\right] \tag{26}$$

Absorber Plate Exergy

The exergy balance of the absorber plate is:

$$\begin{aligned} Ex_{dest,\ Absorber} = \ & \alpha_p\tau_g Ex_{sun} - Ex_{r,p-g} - Ex_{c,p-g} \\ & -Ex_{cond,p-a} - Ex_{c,p-f} \end{aligned} \tag{27}$$

where $Ex_{cond,p-a}$ is the conductive exergy transferred from the absorber plate to the surroundings and given as:

$$Ex_{cond,p-a} = \frac{k_i}{\delta_i} S_p (T_p - T_a) \left(1 - \frac{T_a}{T_p}\right) \tag{28}$$

and $Ex_{c,p-f}$ is the convective exergy transferred from the absorber plate to the working fluid and expressed as:

$$Ex_{c,p-f} = h_{c,p-f} S_{ech} (T_p - T_f) \left(1 - \frac{T_a}{T_p}\right) \tag{29}$$

Working Fluid Exergy

The exergy balance of the working fluid is written as [35,36]:

$$Ex_{d,f} = h_{c,p-f} S_{ech} (T_p - T_f) \left(1 - \frac{T_a}{T_p}\right) - \dot{m}_f C_{p,f} \left[(T_{out} - T_{in}) - T_a ln \left(\frac{T_{in}}{T_{out}}\right)\right] \tag{30}$$

Solar Collector Exergy Efficiency

The exergy efficiency (η_{ex}) of the flat-plate solar collector is defined as the ratio of exergy gained by the working fluid to the exergy input to the SAH [37].

$$\eta_{ex} = \frac{\dot{m}_f C_{p-f} \left[T_{out} - T_{in} - T_a ln \left(\frac{T_{out}}{T_{in}}\right)\right]}{G S_{col} \left[1 + \frac{1}{3}\left(\frac{T_a}{T_s}\right)^4 - \frac{4}{3}\left(\frac{T_a}{T_s}\right)\right]} \tag{31}$$

EXPERIMENTAL ERROR ANALYSIS

The approach given by Holman [38] is adopted, to calculate the error in the acquired results. The proportion error of the solar air heater system efficiency is calculated as:

$$W_S = \left[\left(\frac{\partial S}{\partial x_1} W_1\right)^2 + \left(\frac{\partial S}{\partial x_2} W_2\right)^2 + \cdots + \left(\frac{\partial S}{\partial x_n} W_n\right)^2\right]^{1/2} \tag{32}$$

From the equation of thermal efficiency (η), the uncertainty of efficiency can be derived (following Eq. (19)) as:

$$W_\eta = \left[\left(\frac{\partial \eta}{\partial \Delta T} W_{\Delta T}\right)^2 + \left(\frac{\partial \eta}{\partial m} W_m\right)^2 + \left(\frac{\partial \eta}{\partial A_p} W_{A_p}\right)^2 + \left(\frac{\partial \eta}{\partial I} W_I\right)^2\right]^{1/2} \tag{33}$$

The uncertainties of measured and resulting data are shown in Table 1.

Table 1. Uncertainties of measured and resulted data

Parameter	Uncertainty
Air temperature difference	±2.3 (℃)
Mass flowrate ($\dot{m}_{air}$)	±0.03 (kg/s)
Solar radiation	±1.6 (W/m^2)
Heater area	±0.8 (m^2)
Thermal efficiency	±3.5 (%)

RESULTS AND DISCUSSION

The experimental measurements are carried out from (12/2/2019) to (14/5/2019) in clear sky conditions. The results are presented for three air velocities of 1.9 m/s, 1.7 m/s, and 0.9 m/s. The measurements are carried out for 10 hours /day under almost clear sky conditions to minimize the effect of the cloud on direct solar radiation.

Figure 6 shows the solar radiation intensity distribution with local time for all the experiment days. The solar intensity rises gradually from the early hours of the day to a peak value at noon and then falls during the day. For the 12-May, the solar intensity is 409 W/m^2 at 8:00 h and increases to reach 918 W/m^2 at 12:00, and then it reduces from afternoon until sunset. Calculating the average solar intensity for all the experiments days reveals that the average daily values of solar intensity can be approximately considered as stable as it ranges between 440 W/m^2 and 346 W/m^2.

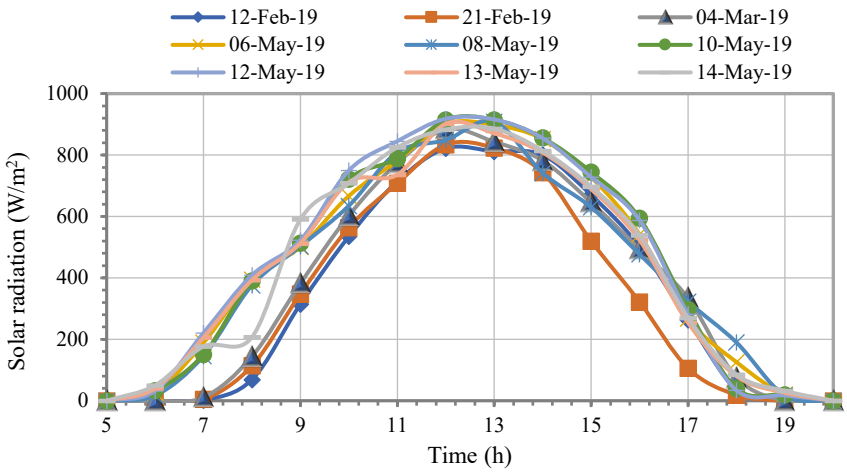

Figure 6. The hourly variation of solar irradiance

Figure 7(a) to 7(c) show the temperature profiles of the absorber plate and air versus time for the SAH with smooth absorber plate for the velocities 1.9 m/s, 1.7 m/s and 0.9 m/s, respectively. In general, the temperatures of plate, air inlet and air outlet were found to be rising exponentially from the early morning to reach the maximum values at noon and then fall gradually during the day with some fluctuations through some days. The maximum air temperatures at the exit are 48 ℃, 49 ℃ and 52 ℃ for velocities of 1.9 m/s, 1.7 m/s and 0.9 m/s, respectively. This means that the lower air velocity, the higher air temperature. This behavior can be rationalized as, at low velocity the air spends more time in contact in the upper and lower pass of the double-pass solar air heater.

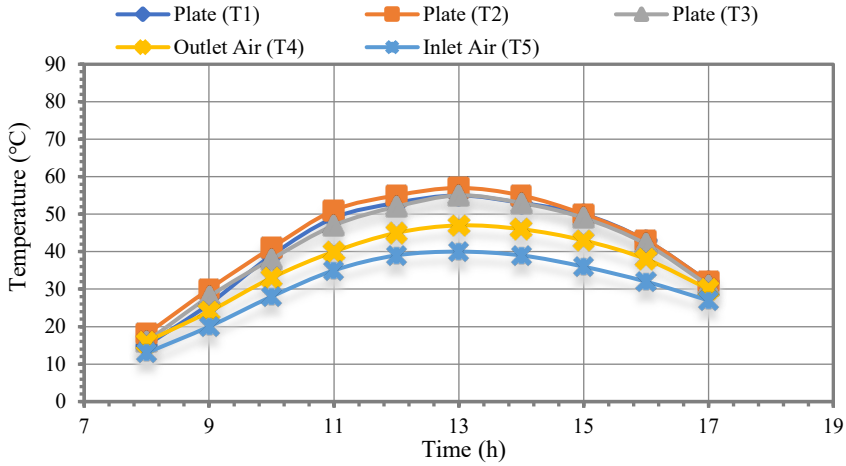

(a) at v=1.9 m/s (on 12-Feb-2019)

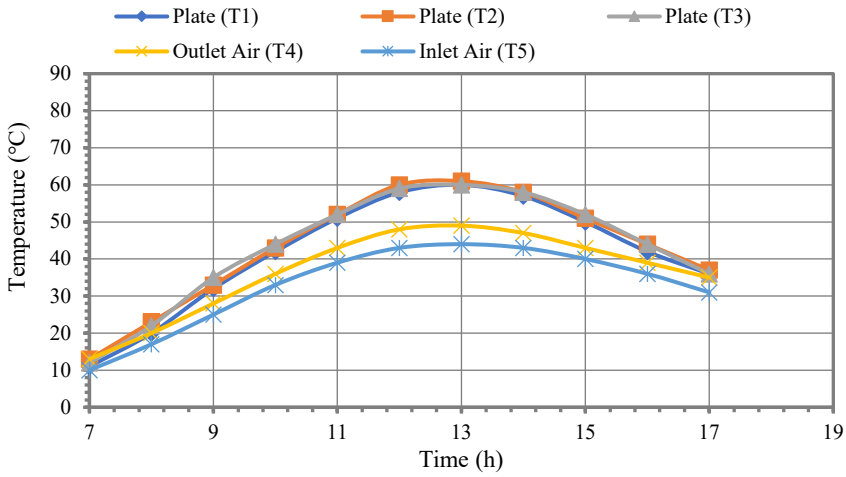

(b) at v = 1.7 m/s (on 21-Feb-2019)

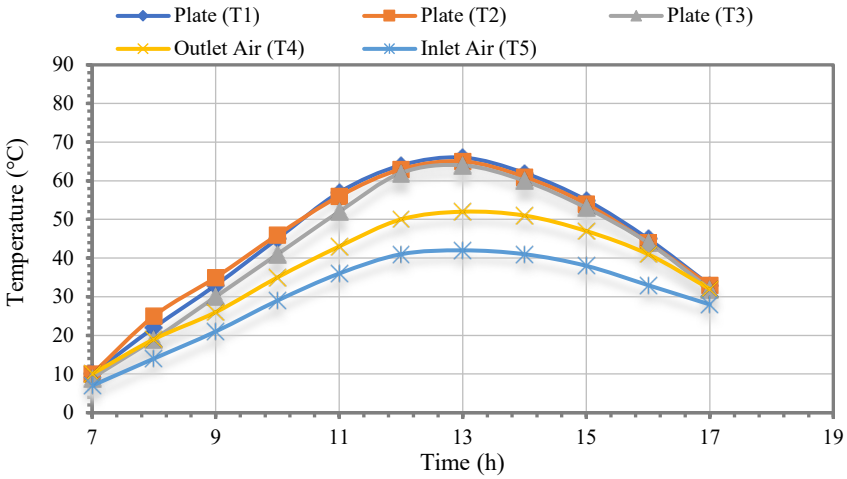

(c) at v = 0.9 m/s (on 4-March-2019)

Figure 7. The hourly variation of temperatures inside the solar air heater without fins

Figures 8(a) to 8(c) show the temperature profiles of the absorber plate and air versus time for the SAH with one line of fins (6 fins) - absorber plate for the velocities of 1.9 m/s, 1.7 m/s and 0.9 m/s respectively. The effect of fins on the air temperature at the exit is clear as the air maximum temperature increased from 48 °C, 49 °C and 52 °C for a smooth plate to 50 °C, 52 °C and 57 °C of an online finned plate at velocities of 1.9 m/s, 1.7 m/s and 0.9 m/s, respectively. The increase is attributed to the increased surface area of the absorber plate and the generated turbulence. The comparison between the maximum air temperature for different days is justified because the range of the variation of average solar intensity is small.

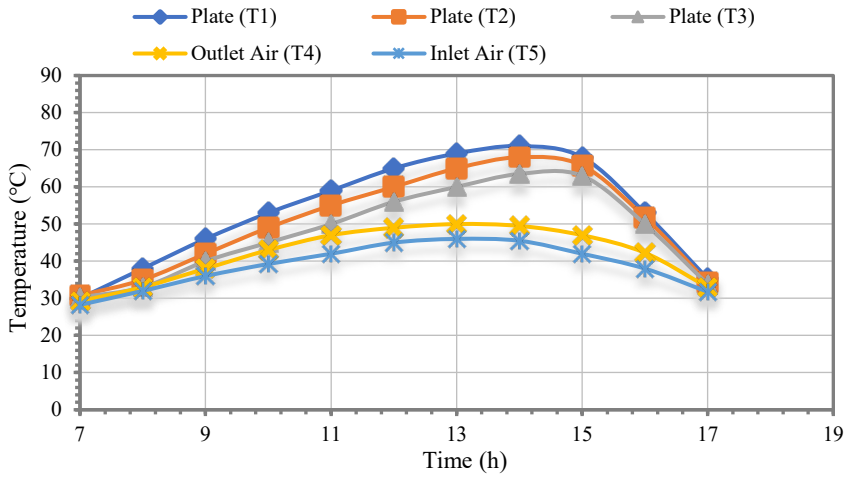

(a) at v=1.9 m/s (6-May-2019)

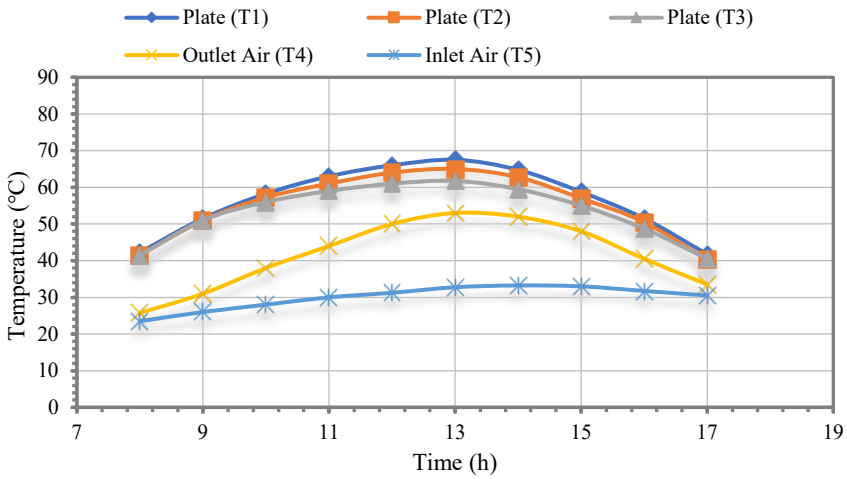

(b) at v=1.7 m/s (on 8-May-2019)

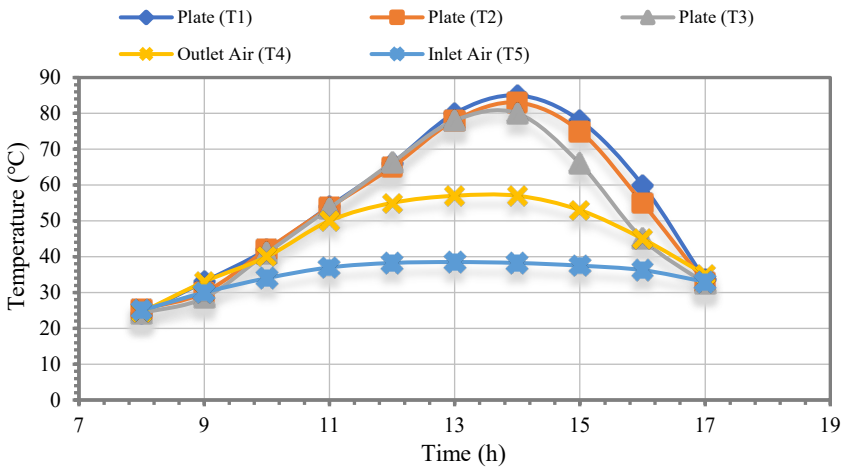

(c) at v=0.9 m/s (on 10-May-2019)

Figure 8. Hourly variation of temperatures inside the solar air heater in case of one line of fins

Figure 9(a), 9(b) and 9(c) show the temperature profiles of the absorber plate and air versus time for the SAH with two lines of fins (12 fins) - absorber plate for the velocities of 1.9 m/s, 1.7 m/s and 0.9 m/s. The effect of two lines of fins on the air temperature at the exit is more significant as the air maximum temperature increased from 50 °C, 52 °C and 57 °C for one line finned plate to 56.5 °C, 58.5 °C and 64 °C for two lines finned plate for velocities of 1.9 m/s, 1.7 m/s and 0.9 m/s respectively. This greater effect of the fins on the temperature of the air for two lines of fines is attributed to the larger surface area and the larger turbulence generation rate due to the greater fin number.

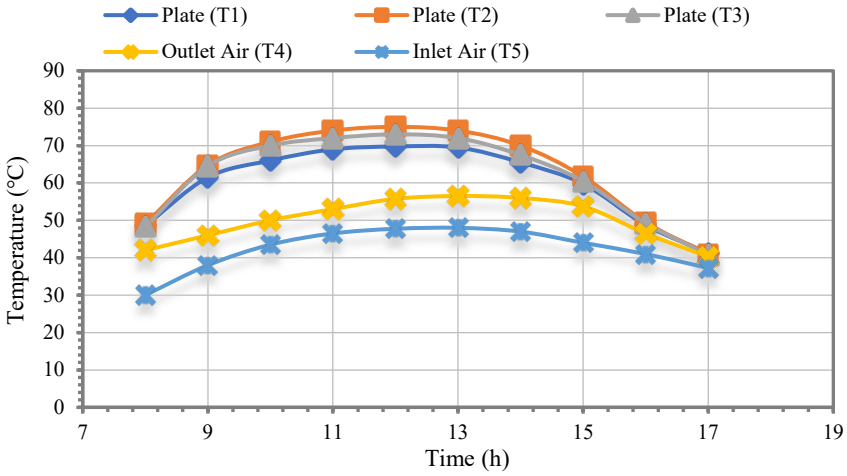

(a) at v=1.9 m/s (on 12-May-2019)

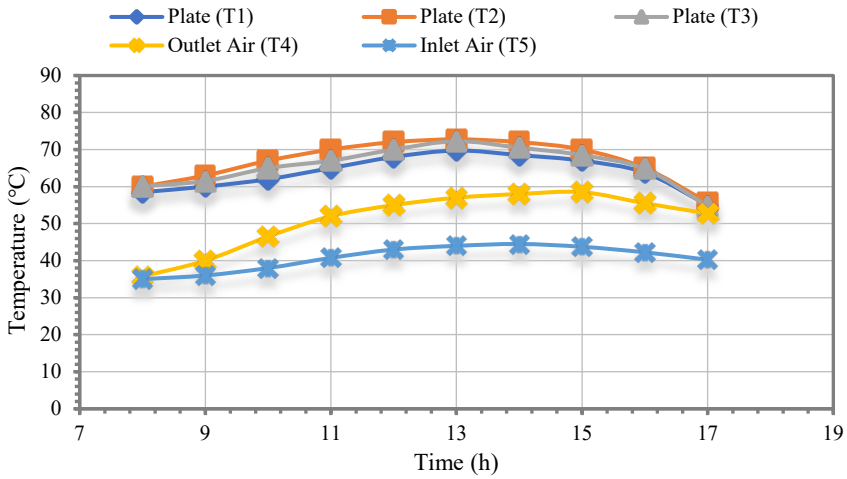

(b) at v=1.7 m/s (on 13-May-2019)

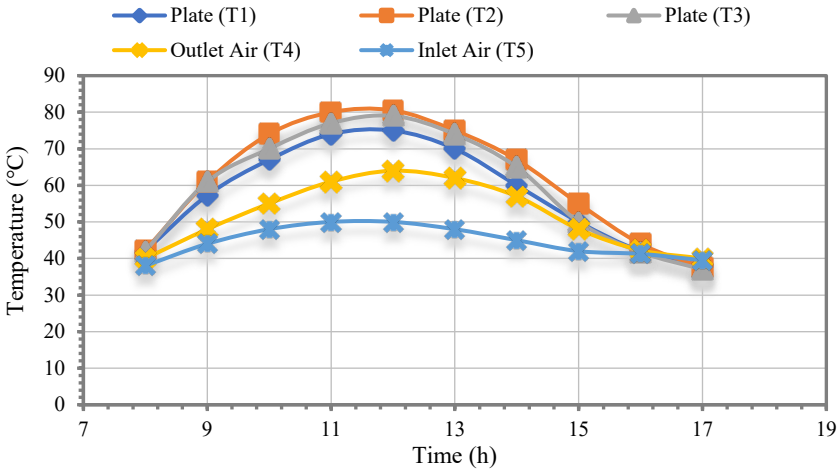

(c) at v=0.9 m/s (on 14-May-2019)

Figure 9. Hourly variation of temperatures inside the solar air heater in case of two lines of fins

Efficiency Variation with Time of the Day

Efficiency variation of the double pass solar air heater with local time at various air velocities for smooth, one line of fins and two lines of fines absorber plate is shown in Figures 10(a) to 10(c). The efficiencies increase from the early of the day to reach the maximum values at 13:00 h and then decrease gradually; this is because the efficiency is a function of solar intensity. The efficiency is strongly affected by the presence of the fins on the absorber plate. For the velocity of 1.9 m/s the average efficiency is enhanced by 28% and 66% for one line and two lines of fins, respectively, as compared with the efficiency of the smooth plate. For the velocity of 1.7 m/s, the average efficiency is enhanced by 27% and 51% for one line and two lines of fins, respectively, as compared with the efficiency of the smooth plate. For the velocity 0.9 m/s the average efficiency is enhanced by 21% and 50% for one line and two lines of fins, respectively, as compared with the efficiency of the smooth plate. These results indicate that introducing fins to the double-pass air solar heater improves the average efficiency by 21% to 66% for the current experiment conditions. To validate the obtained results, a comparison of efficiency of previously tested SAHs in literature and the present solar air heater is given in Table 2. The efficiency of present work exhibits a good agreement with those from the literature.

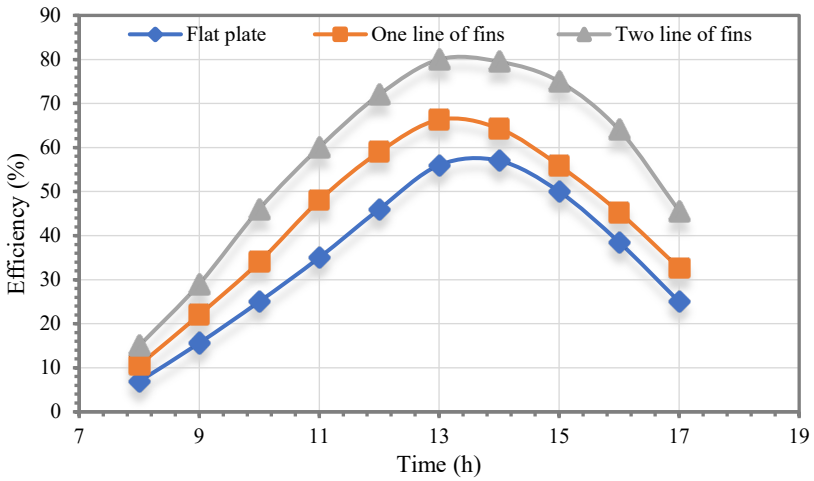

(a) at v = 1.9 m/s

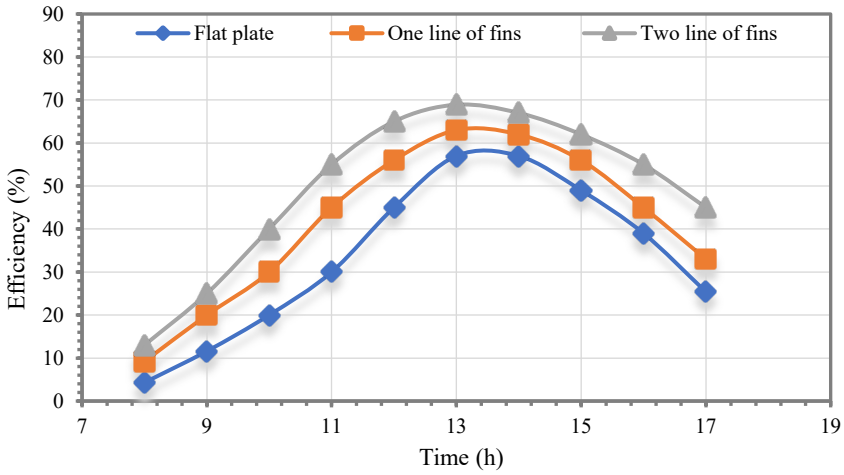

(b) at v =1.7 m/s

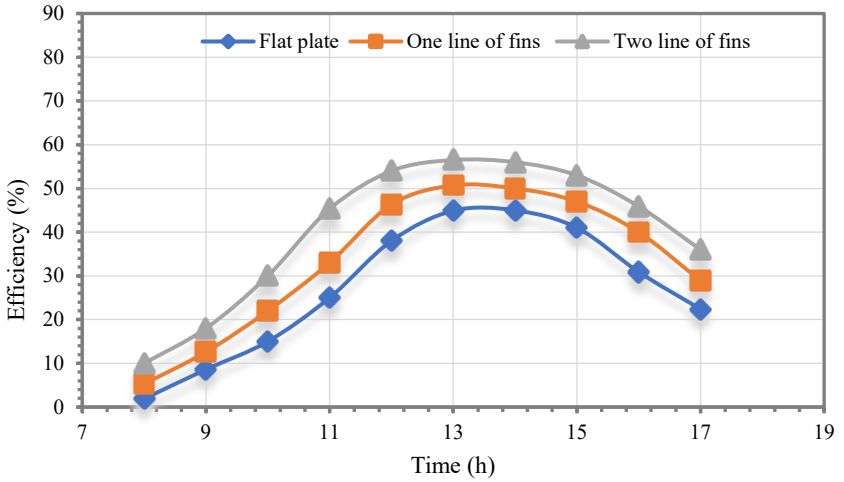

(c) at v=0.9 m/s

Figure 10. The hourly variation of thermal efficiency for solar air heater

Daily Variation in Components Exergy Destruction Rates

The rate of exergy destruction is calculated for the solar air heater's components with two lines of fins: the absorber plate, glass cover, and working fluid, and the results for various velocities (v= 1.9 m/s, 1.7 m/s, and 0.9 m/s) are shown in Figures 11(a) to 11(c). Exergy destruction rates are related to solar intensity, where the greatest point of exergy destruction rate occurs at the maximum solar intensity. Exergy destruction rates for glass cover and working fluid are low as compared to those for absorber plate due to tiny temperature variations. Figure 11 prove clearly that the exergy destruction rate increases for all components of the solar air heater with increasing velocity due to increasing the output air temperature with increasing velocity. The average exergy destruction rate in the absorber plate, working fluid, and glass cover increased by 15.76%, 33.99%, and 38.57%, respectively, for velocity increase from 0.9 m/s to 1.7 m/s. It increased by 18.88%, 19.8%, and 21.65% for absorber plate, working fluid, and glass cover, respectively as velocity increase from 1.7 m/s to 1.9 m/s.

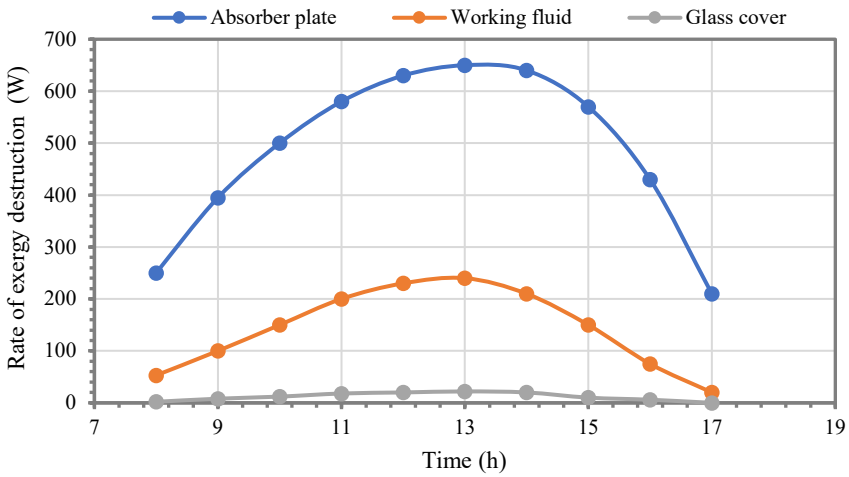

(a) at v = 1.9 m/s (on 12-May-2019)

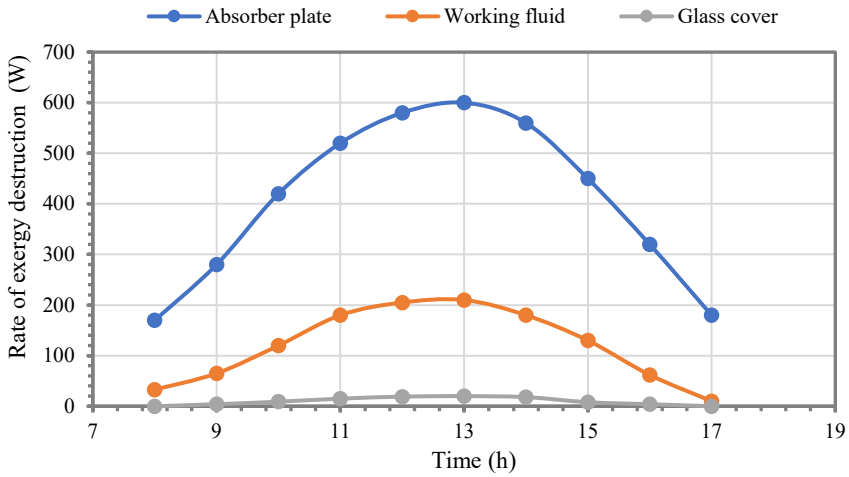

(b) at v = 1.7 m/s (on 13-May-2019)

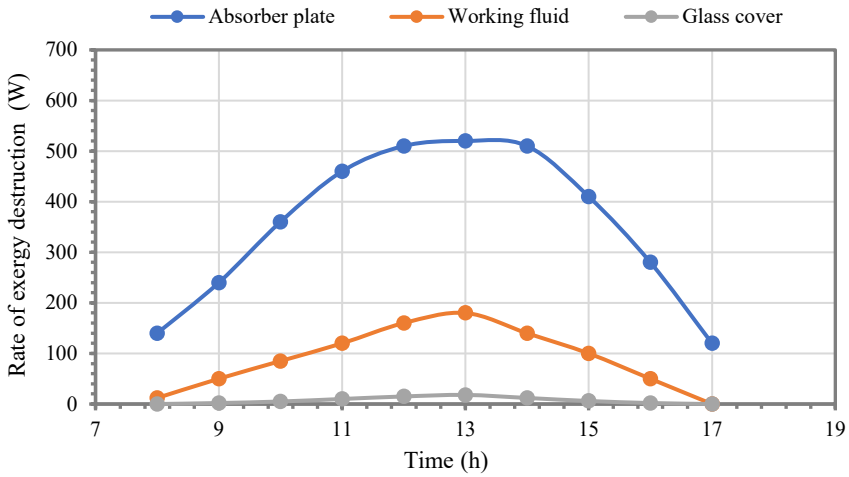

(c) at v = 0.9 m/s (on 14-May-2019)

Figure 11. Hourly variation of exergy destruction rates in the absorber plate, working fluid, and glass cover

The variance in exergy efficiency for different velocities can be seen in Figure 12. The efficiency of the solar air heater increases with increasing velocity, which is due to an increase in the temperature of the outlet air, which increases with increasing velocity. Exergy efficiency increased by 10.34% when the velocity was increased from 0.9 m/s to 1.7 m/s, and it increased by 12.5% when the velocity was increased from 1.7 m/s to 1.9 m/s.

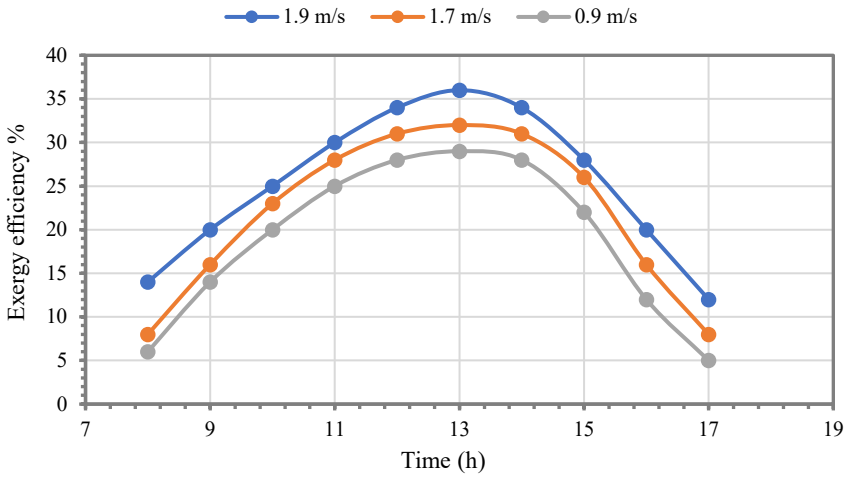

Figure 12. Hourly variation of exergy efficiency at different air velocities

Table 2. Comparison of other studies with the current study

Type of solar air heater	Ref.	Site location	Thermal efficiency (%)
Present study		Iraq	80
Single-pass solar air heater with reflectors and turbulators	[13]	Saudi Arabia	78
Tubular solar heater (TSAH)	[16]	Egypt	84
Solar air heater with (S) shaped ribs with gap	[17]	China	65
Arc-shaped roughened solar air heater	[18]	India	76
Triple-pass solar air heater	[19]	Iraq	80.2
Solar air collectors with different delta turbulators arrangement	[39]	Iraq	88

CONCLUSIONS

A single line (6 fins) and two lines (12 fins) effect (of L shape fins fix) on the upper face flat absorber plate on the thermal performance of a double-pass solar air heater is investigated experimentally under the weather condition of Baghdad, Iraq. The main conclusions from this work can be summarized as follows:

i. The temperature of the solar air heater is a function of solar intensity, flow velocity and absorber plate configuration.
ii. For the smooth absorber plate, the maximum air exit temperature increases from 48 °C to 52 °C as the velocity decreases from 1.9 m/s to 0.9 m/s.
iii. For the absorber plate with one line of fins, the maximum air exit temperature increases from 50 °C to 57 °C as the velocity changes from 1.9 m/s to 0.9 m/s.
iv. For the absorber plate with two lines of fins, the maximum air exit temperature increases from 56.5 °C to 64 °C as the velocity changed from 1.9 m/s to 0.9 m/s
v. The presence of the fins improve the efficiency due to the increased surface area and the generated turbulence.
vi. Using one line of fins improves the average efficiency by 21% to 28% for the velocity change from 0.9 m/s to 1.9 m/s.
vii. Using two lines of fins improves the average efficiency by 50% to 66% for the velocity change from 0.9 m/s to 1.9 m/s.
viii. The average exergy destruction rate increased by 37.6%, 60.6%, and 68.66% for absorber plate, working fluid, and glass cover, respectively, when the velocity increased from 0.9m/s to 1.9m/s.
ix. Exergy efficiency increased by 24.1% when the velocity increased from 0.9m/s to 1.9 m/s.

ACKNOWLEDGEMENT

The authors acknowledge the technical support provided by the staff of Air Conditioning and Refrigeration Center at Al-Esraa university college.

REFERENCES

[1] S. Rashidi, M.H. Kashefi, and F. Hormozi, "Potential applications of inserts in solar thermal energy systems – A review to identify the gaps and frontier challenges," *Solar Energy*, vol. 171, no. September, pp. 929-952, 2018.
[2] A. Gilani , S. Hoseinzadeh, "Techno-economic study of compound parabolic collector in solar water heating system in the northern hemisphere," *Applied Thermal Engineering*, vol. 190. no. May, pp. 116756, 2021.

[3] S. Rashidi, F. Hormozi, B. Sundén and O. Mahian, "Energy saving in thermal energy systems using dimpled surface technology – A review on mechanisms and applications," *Applied Energy*, vol. 250, no September, pp. 1491-1547, 2019.

[4] K. Manikandan , S. Iniyan and R. Goic, "Enhancing the optical and thermal efficiency of a parabolic trough collector – a review," *Applied Energy*, vol. 235, no. February, pp. 1524– 1540, 2019.

[5] L. Meng, W. Zhang, D. Quan, G. Shi, L. Tang *et al.*, "From topology optimization design to additive manufacturing: today's success and tomorline's roadmap," *Archives of Computational Methods in Engineering*, vol. 27, no. July, pp. 805–830, 2019.

[6] X. Zhao, E. Jiaqiang, Z. Zhang, J. Chen, G Liao *et al.*, "A review on heat enhancement in thermal energy conversion and management using Field Synergy Principle," *Applied Energy*, vol. 257, no. January, pp. 113995, 2020.

[7] J. Choi, and J. Eastman, "Enhancing thermal conductivity of fluids with nanoparticles," *ASME International Mechanical Engineering Congress & Exposition*, vol. 231, no. October, pp. 99-105, 1995.

[8] M. Sms, and A. Castro, *Nanofluids: synthesis, properties and applications,* New York: Nova Science Publishers Inc, 2014.

[9] S. Murshed and D. Castro "A critical review of traditional and emerging techniques and fluids for electronics cooling," *Renewable and Sustainable Energy Reviews*, vol. 78, no. October, pp. 821–33, 2017.

[10] M. Al-Dulaimi, A. Rasool, and F. Hamad, "Investigation of impingement heat transfer for air-sand mixture flow," *The Canadian Journal of Chemical Engineering*, vol. 94, no. January, pp.134-141, 2016.

[11] P. Kumar, K. Panchabikesan, L. Deeyoko and V. Ramalingam, "Experimental investigation on heat transfer augmentation of solar air heater using shot blasted V-corrugated absorber plate," *Renewable Energy*, vol. 127, no. Novemver, pp.213-229, 2018.

[12] B. Jiaa, F. Liu, D. Wang, "Experimental study on the performance of spiral solar air heater," *Solar Energy*, vol. 182, no. April, pp.16–21, 2019.

[13] A. Abdullah, M. Amro, M. Younes, Z. Omara, A. Kabeel and F. Essa, " Experimental investigation of single pass solar air heater with reflectors and turbulators," *Alexandria Engineering Journal*, vol. 59, no. April, pp.579–587, 2020.

[14] D. Dezan, A. Rocha, and W. Ferreira, " Parametric sensitivity analysis and optimization of a solar air heater with multiple lines of longitudinal vortex generators," *Applied Energy*, vol. 263, no. April, pp.114556, 2020.

[15] N. Jouybari, and T. Lundström, "Performance improvement of a solar air heater by covering the absorber plate with a thin porous material," *Energy*, vol. 190, no. January, pp. 116437, 2020.

[16] H. Hassan, and S.Abo-Elfadland M. El-Dosoky, "An experimental investigation of the performance of new design of solar air heater (tubular) ," *Renewable Energy*, vol. 151, no. May, pp. 1055-1066, 2020.

[17] D. Wanga, J. Liu, Y. Liu, Y. Wang, L. Bojia, and J. Liu, "Evaluation of the performance of an improved solar air heater with "S"shaped ribs with gap," *Solar Energy*, vol. 195, no. January, pp.89–101, 2020.

[18] H. Ghritlahrea, P. Sahu, and S. Chand, "Thermal performance and heat transfer analysis of arc-shaped roughened solar air heater – An experimental study," *Solar Energy*, vol. 199, no. March, pp. 173–182, 2020.

[19] H. Yassien, O. Alomar, and M. Salih, "Performance analysis of triple-pass solar air heater system: Effects of adding a net of tubes below absorber surface," *Solar Energy*, vol. 207, no. September, pp. 813–824, 2020.

[20] M. Baissia, A. Brimaa, K. Aouesa, R. Khanniche, and N. Moummi, "Thermal behavior in a solar air heater channel roughened with delta-shaped vortex generators," *Applied Thermal Engineering*, vol. 165, no. January, pp.113563, 2020.

[21] S. Hosseini, A. Ramiar, and A. Ranjbar, " Numerical investigation of natural convection solar air heater with different fins shape," *Renewable Energy*, vol. 117, no. March, pp. 488-500, 2018.

[22] S. Hosseini, A. Ramiar, and A. Ranjbar, "Thermo-hydraulic performance of a solar air heater with staggered C-shape finned absorber plate," *International Journal of Thermal Sciences*, vol. 168, no. October, pp. 107068, 2021.

[23] H. Olia, M. Torabi, M. Bahiraei, M. Ahmadi, M. Goodarzi, and M. Safaei, "Application of nanofluids in thermal performance enhancement of parabolic trough solar collector: state-of-the-art," *Applied Sciences,* vol. 9, no. January, pp. 1-22, 2019.

[24] S. Rashidi, P. Javadi, and J. Esfahani, "Second law of thermodynamics analysis for nanofluid turbulent flow inside a solar heater with the ribbed absorber plate," *Journal of Thermal Analysis and Calorimetry*, vol. 135, no. March, pp. 551-563, 2019.

[25] S. Hoseinzadeh, S. Otaghsara , M. Khatir and P. Heyns, "Numerical investigation of thermal pulsating alumina/water nanofluid flow over three different cross-sectional channel," *International Journal of Numerical Methods for Heat & Fluid Flow*, vol. 30, no. 7, pp. 3721-3735, 2019.

[26] J. Duffie and W. Beckman, *Solar engineering thermal processes,* New York: John Wiley & Sons, 2013.

[27] P. Matuszewski, and M. Sawicka, *Optimization of solar air collector*, Aalborg: Aalborg University, 2010.

[28] F. Incropera and D DeWitt, *Introduction to heat transfer*, New York: John Wiley & Sons, Inc., 2002.

[29] E. Alfegi, K. Sopian, M. Othman, and B. Yatim, "Mathematical model of double pass photovoltaic thermal air collector with fins," *American Journal of Environmental Sciences*, vol. 5, no. October, pp.592-598, 2009.

[30] M. Moran and H. Shapiro, *Fundamentals of engineering thermodynamics*, SI Version, 6th ed. New Delhi: Wiley India (P) Ltd, 2010.

[31] R. Petela, *Engineering thermodynamics of thermal radiation: For solar power utilization*, New York: McGraw Hill, 2010.

[32] A. Bejan, *Advanced engineering thermodynamics*, Hoboken: Wiley, 2006.

[33] R. Petela, "Exergy of heat radiation," *ASME Journal of Heat and Mass Transfer,* vol. 2, no. May, pp. 187–192, 1964.

[34] R. Petela, "Exergy analysis of the solar cylindrical-parabolic cooker," *Solar Energy*, vol. 79, no. September, pp. 221–233, 2005.

[35] M. Karakilcik and I. Dincer, "Exergetic performance analysis of a solar pond," *International Journal of Thermal Sciences,* vol. 47, no. January, pp. 93–102, 2008.

[36] A.Dehghan, A. Movahedi, and M. Mazidi, " Experimental investigation of energy and exergy performance of square and circular solar ponds," *Solar Energy*, vol. 97, no. November, pp. 273–284, 2013.

[37] N. Singh, S. Kaushik and R. Misra, " Exergetic analysis of a solar thermal power system," *Renewable Energy*, vol. 19, no. January, pp. 135–143, 2000.

[38] J. Holman, *Heat Transfer*, New York: McGraw Hill Higher Education, 2010.

[39] Z. Obaid, A. Al-damook and W. Khalil, "The thermal and economic characteristics of solar air collectors with different delta turbulators arrangement," *Heat Transfer, Asian Research*, vol. 48, no. May, pp. 2082-2104, 2019.